File with Technical Note E.

HYDRAULICS DIVISION

Technical Note

CCIW
JUN 18 1984
c.2
LIBRARY

DATE: January 1984 **REPORT NO:** ESS-83

TITLE: Electro-optical Performance Review of a Flume Profiler Fiber Optic-Probe

AUTHOR: R.J. Desrosiers

REASON FOR REPORT: To partially fulfill requirements of Study 327.

CORRESPONDENCE/STUDY NO: 83-389(327)

ABSTRACT

A fibre optic flume profiler was built under contract. A review of the electro-optical performance of the probe was requested due to problems noted in the use of the sensor. The sensor was found to be sensitive to bottom reflectance and ambient light. Circuit calculations were performed which indicated that the adjustment span was less than that required and that the sensor was sensitive to temperature variations but within error tolerances in this respect. This note describes the measurements and calculations performed to characterize the sensor. Conclusions and recommendations were given.

1.0 INTRODUCTION

The probe studied was manufactured by Metrex Instruments of Toronto. The specific problems noted by the NWRI lead engineer Mr. A.S. Watson were:

1) It appeared that the "stand-off" distance was dependent on the bottom type.
2) It appeared that the sensor was responsive to ambient light.
3) Design data was essentially non-existent which prevented an understanding of the device operation.

With a view to addressing the above concerns, the author was given the task, within specific time constraints, of analysing the sensor performance and performing measurements of the device outputs. Additionally, recommendations on the use of the sensor were to be provided.

This note reports on these results and analyses.

2.0 SENSOR IDEALIZED RESPONSE

Mr. Watson suggested that the idealized desired response of the sensor which is illustrated in Figure 1 would be that shown in Figure 2. The sensor or at least the error signal to the servo would have a response with a negative slope and clipped at the top and bottom. Elementary considerations indicate that this is likely correct. If the probe is far away the clipped levels set the probe toward the null at a constant rate. When the probe reaches a point where the signal is a linear function of distance a null will be sought by the servo. Analysis of the servo was beyond the terms of

reference of this study but the idealized servo error signal should be borne in mind in the discussion which follows.

3.0 MEASUREMENTS

3.1 Sensor Output Versus Distance for Various Targets

The sensor output as a function of distance from the probe tip was measured using various targets simulating various flume bottoms. The probe assembly was mounted on an optical bench. A target was mounted on a 90 degree angle mount which in turn was attached to a micrometer driven slide (with adjustments to 200 microinches). This target assembly was in turn mounted on the optical bench co-linearly with the probe shaft. The targets used were:

1) Barium sulfate white target with 99% diffuse reflectance
2) 40 grit alumide cloth
3) 80 grit aluminum oxide paper
4) 100 grit garnet paper
5) 135 grit emery cloth (black).

The sensor pre-amp output (pins H and A of the hex connector) and the buffer amp output (ICI pin 7 and hex connector pin A) were measured. These were measured using a Hewlett-Packard 59306A relay actuator acting as a multiplexer and a HP 3490A multimeter. These instruments were controlled using an IEEE-488 bus and a HP 9845 desktop computer. At each position approximately 32 measurements were taken. The mean and the standard deviation were computed. The output of the pre-amp and the buffer amp were plotted as a function of distance from the probe tip. All measurements were done under "zero" ambient light except where noted.

The results are illustrated by Figures 3 through 8. These clearly show that the instrument is sensitive by an order of magnitude or more to simulated bottom type. Note that the white target was used to simulate the white glass bead bottoms occasionally used and the black target was used to simulate the SiC material again sometimes used. Since the instrument is based on the measurement of reflected light from the target, the instrument is inherently sensitive to variations in the diffuse reflectance of the bottom. Thus the results were not unexpected. It should be pointed out that the measurements were done in air. The absolute magnitude of the tests cannot be directly applied to submersed targets. It is, however, the relative change in the sensor response to target type which should be noted.

The results for the 135 grit black emery cloth were too near the noise limit for adequate detection and the results are not shown.

3.2 The Effects of Ambient Light

The ambient illumination above a number of flumes in the hydraulics laboratory was measured using a Tektronics J16 digital photometer with a cosine corrected illuminance probe. The values found were between 400 and 500 lux except for one or two areas above a smaller flume which had additional fluorescent fixtures where the illumination was about 1000 lux. The lower values are within the Illumination Engineering Society guidelines where fine detailed work is not done.

The flume profiler amplifier output versus distance was measured under dark and under ambient light illuminance of approximnately 480 lux fluorescent light for 80 grit paper target as an example. The output variations were equivalent to about 2 mm in

the linear region of the response curve. This probably would not be too excessive for a probe of this type. However, the effects of a red filter (Rosco #832) were measured using the same sets of conditions as without the filter. The filter reduced the effect in the linear region to the noise level and was only apparent in distances far from the probe. See Figures 9 through 12. It must be pointed out that these reductions would only apply to fluorescent or metal halide ambient lighting and most definitely not be applicable to tungsten, i.e., incandescent illumination.

3.3 Zero Noise and Drift

The probe output using a black target very far away was determined. This was found to be 2mV +/- 0.2mV for the preamp and 5 mV for the buffer amp output (one sigma or one standard deviation). These were low frequency measurements.

The drift over 20 minutes at one spacing was about two to three standard deviations.

The power line noise was not measured with the system power supply and buffer amplifier and cable since these were required for other uses before measurements were possible. Using a separate power supply (an Anatek model 515E) 6 mv peak to peak 60Hz noise was measured with a very distant target.

3.4 Source Beam Divergence

The source beam divergence was measured by mounting the probe on the optical bench and then measuring the observable beam diameter at various distances from the probe tip. The beam divergence was found to be approximately 40 degrees full width in the air. It is

easy to show that to the first order the beam divergence in water would be the beam divergence in air divided by the refractive index of water, i.e., 40/1.33 = 30 degrees. The initial beam size was measured to be about 5 mm. The distance from the probe tip which generally had the maximum linearity was about 5 mm from the probe tip. Thus the beam size at 5 mm distance would be 2 x (2.5 + 5 tan (15)) = 7 to 8 mm wide. This width would be the measurement diameter on the bottom. This puts an effective limit to the spatial frequency and magnitude of bottom ripples to a value of 1/4 to 1/5 of this to ensure that peaks in the ripples do not hit the probe tip.

3.5 Source Irradiance

The source power was measured using an Alphametrics DC1010 radiometer using a flat response probe #203 and was found to be approximately five microwatts.

3.6 Fibre Size

The fiber size was 0.01 inches or 250 micrometers. The diameter of the entire bundle was 5 mm. Thus there were about 400 fibres in the bundle for both the source and receiver.

4.0 CIRCUIT ANALYSIS

The circuit schematic of the sensor pre-amp and the buffer amplifiers was provided by Mr. Watson. Mr. Watson requested that the fiber optic probe parts of the Metrex Schematic 203-2-3 be analyzed.

4.1 First Stage Amplifier or Pre-Amp

The schematic is shown below.

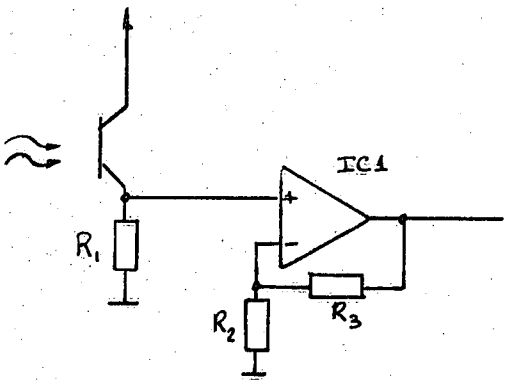

IC1;LF351N

This may be modelled simply as

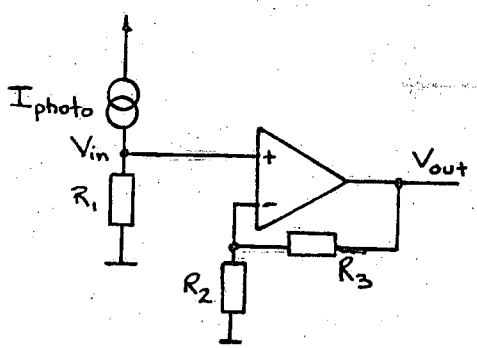

where I (photo) is the photocurrent in the collector (emitter). Thus V(in) = I(photo) x R1. The amplifier is simply a non-inverting gain stage with

$$V(\text{out 1st stage}) = \frac{R2 + R3}{R2} \times V(\text{in}) = \frac{R2 + R3}{R2} \; R1.I\,(\text{photo}).$$

The LF351N has an offset voltage of 1mV maximum and its effect may be modelled as

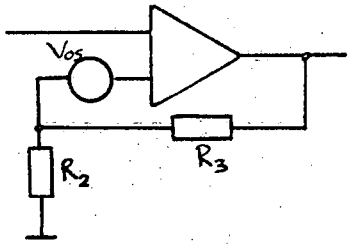

Thus an offset voltage term referred to the output of magnitude $\frac{R_2 + R_3}{R_2}$ Vos is also present. Because the resistance values are low the bias current and offset current may be neglected.

Second and Third Stage Amplifiers

The schematic for these stages is

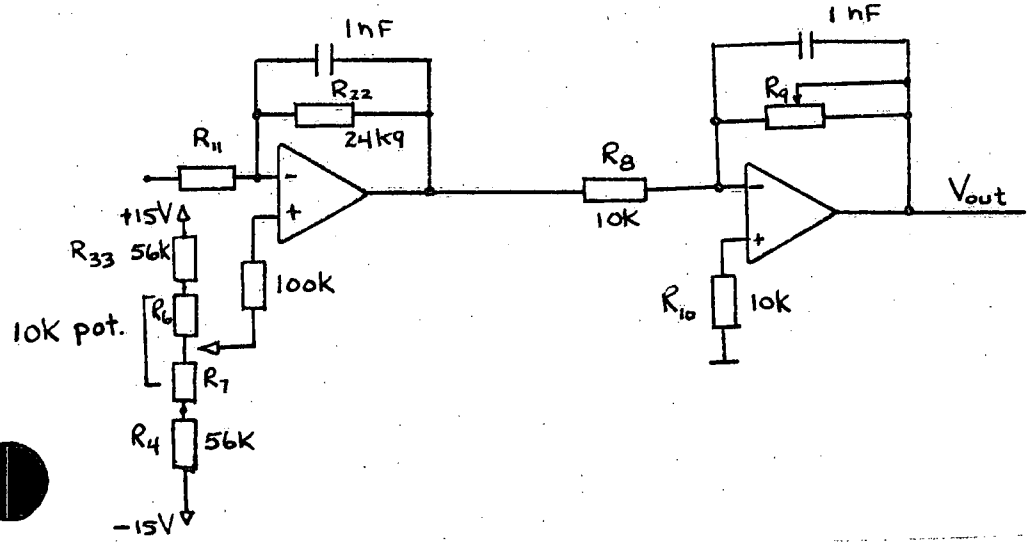

The second stage may be modelled as

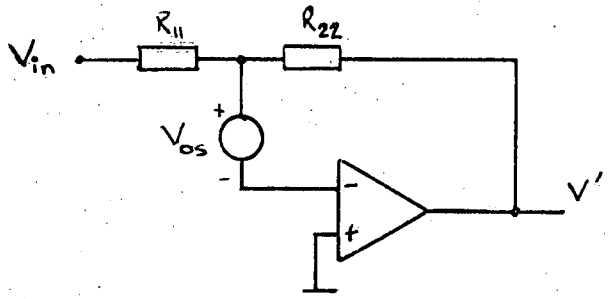

so that after elementary analysis

$$V' = -\frac{R22}{RII} Vin + Vos \left(\frac{R22}{RII} - 1\right)$$

where Vos = Voff + Vampoffset.

The third stage is a similar inverting stage with

$$Vout = -V'\left(\frac{R9}{R8}\right) + Voffset\ of\ 3rd\ stage\ \left(\frac{R9}{R8} - 1\right)$$

On substitution this gives

$$Vout = -(-\frac{R22}{R11} Vin + Vos(\frac{R22}{R11}-1) \frac{R9}{R8} + Voffset\ 3rd\ stage\ (\frac{R9}{R8} -1)$$

$$Vout = \frac{R9}{R8}\frac{R22}{R11} Vin - Vos \frac{R9}{R8} (\frac{R22}{R11} -1) + Voffset\ 3rd\ stage\ (\frac{R9}{R8} -1)$$

Substituting the value for Vin which is the output of the pre-amp stage and for the constituent terms of Vos we get

$$Vout = (\frac{R2 + R3}{R2}) R1 \frac{R9}{R8}\frac{R22}{R11} Iphoto + (\frac{R2 + R3}{R2}) \frac{R9}{R8}\frac{R22}{R11} Voff\ 1st\ op\ amp$$

$$-Voff \frac{R9}{R8} (\frac{R22}{R11} -1)$$

$$-Voffset\ of\ 2nd\ opamp \frac{R9}{R8} (\frac{R22}{R11} -1)$$

$$+Voffset\ of\ 3rd\ stage\ (\frac{R9}{R8} -1)$$

The first term is the desired output. The "Voff" of the third term is adjusted to make the second and fourth terms equal to zero. On substitution the first term is

$$V = \frac{13.3}{3.3} \quad 33 \quad \frac{50}{10} \quad \frac{24.9}{10} \quad Iphoto$$

4.3 Variation of the offset voltage adjustment Voff

The value of Voff is simply found to be

$$Voff = -Vee + (Vcc + Vee) (\frac{R7 + R4}{R33 + R6 + R4})$$

where R6 and R7 are the adjustment pot. parts.

On substitution we have R33 + R6 + R7 + R4 = 122k. The extreme of the offset voltage adjustments are found by setting R7 = 0 and R6 = 10k and then R7 = 10k and R6 = 0. R7 = 0 and R6 = 10k give

$$Voff = -Vee+(Vcc+Vee)(\frac{56}{122}) = -14.7+(15.25.+14.7)(\frac{56}{122}) = -0.95V$$

Similarly, R6 = 0 and R7 = 10k give

$$Voff = -14.7 + (15.25 + 14.7)\frac{66}{122} = 1.50V$$

The sensitivity of this offset adjustment to Vee and Vcc variations are simply found using the data for the line/load regulation of the regulators in the data sheets of the regulator manufacturer. Nominal values are about 150 mV regulation (worst case values are higher, "typical" values are lower). The Vee and Vcc regulators do not track, however. So take the deviation value, i.e., Vee = -14.7 - 0.15 = -14.85V and Vcc = 15.25 + 0.15 = 15.40V. Substituting these values in the extrema equations yield -0.96V in the first case and 1.51 V in the second case. Thus the fluctuation in Voff due to power supply variations is about 10 mV. Using the equation in the previous section transferred to the output this corresponds to

$$0.01\ (\frac{R9}{R8}\frac{R22}{RII} -1) = 0.07V \text{ or a } 70mV \text{ change.}$$

4.4 Temperature Variations of the Amplifiers

The gain equation in Section 4.2 may be used to determine the effects of temperature variations.

The change in the offset voltage of the amplifiers may be determined by substituting the variation in the offset voltage dVos for the offset voltage. Both types of amplifiers have similar temperature coefficients - namely, typically 10 micro volts/°C. Over ±5°C this is ±50 micro volts. Substitution yields ±2.8 mV for the first stage, ±375 micro volts for the second stage, and ±75 micro volts for the third stage.

Because the bias currents are of the order of a few hundred pA and the resistances are small these effects may be neglected.

Similarly temperature variations of the resistors (Phillips MR25 type) are small (tempco ±100 ppm/°C). Because the resistance values are not largely different from each other, the resistances were probably made of the same material and would probably track with respect to each other over temperature. Because the gain is proportional to the ratio of resistances the temperature coefficient variation in each stage should be less than the effect of each individual resistor, i.e., 100 ppm/°C. Because R9 and R10 are not made of the same material they probably would not track. However, over ±5°C this effect would only be about 0.12%.

4.5 Time Variations of the Amplifiers

The time drift of the opamps are not specified but would likely be less than the effects of temperature variations.

4.6 Time Response

In the above calculations the feedback capacitors have been neglected. These feedback capacitors were probably inserted for gain rolloff at higher frequences. The RC product of the third stage is

50×10^{-6} giving a rise time of $t = 2.2RC = 110$ microseconds. The detector itself has a rise time of 18 microseconds. Given the electromechanical nature of the servo the rise time of the amplifiers should probably be raised by an order of magnitude or more by increasing the value of the feedback capacitors.

4.7 Johnson Noise

The amplifier noise in all stages are in themselves essentially negligible. The amplifier input noise in all three stages would be at 10 Hz about 30 nV/Hz. Over a 10 Hz bandwidth this would result in a noise of 3 microvolts. Referred to the output this results in a noise of 240 microvolts. This noise must be multiplied by the same gain values as in the temperature effects of the offset voltage but the initial coefficient is over an order of magnitude smaller. The "noise" evident would almost certainly be governed by fluctuations in the actual detector and/or source drift or cabling.

5.0 DETECTOR RESPONSE

The FPT120 is a Fairchild phototransistor with a dark current of 100 nA and minimum photocurrent of 400 microamps for a light level of 20 mW/sq cm - detecting a tungsten bulb at 2850 K. The saturation current is 1 mA which occurs at a light level of 20 mW/sq cm. It should be pointed out that the device is not linear over the entire dynamic range. However, the linearity is probably of the order of 20% over four decades of irradiance variation which is probably adequate for a servo type system. For the 100 nA maximum dark current

using the gain equation (see Section 3.2) referred to the output one has the noise voltage due to the photocurrent noise or

$$V = \frac{10 + 3.3}{3.3} 33000 \frac{50}{10} \frac{24.9}{10} 100 \times 10^{-9} = 160 \text{ millivolts.}$$

If the "typical" noise current of 10 nA is used instead the noise is 16 mV. The actual measured noise was less than this although the effective measurement bandwidth was only .08 Hz.

However, it appears that the detector noise would swamp opamp and resistor noise in any event.

The photocurrent gain or responsivity appears to follow an exponential variation with temperature. Using the manufacturer's response curves at different temperatures for an illuminance of approximately 0.0157 mW/sq cm a least squares fit determined that the responsivity R[mA] varied with temperature T in °C as

$$R = 0.0235 \exp (0.0326T).$$

Thus at 20°C, 25°C and 30°C the responsivity was calculated to be 0.0451, 0.0530 and 0.0625 mA, respectively. Thus a variation of ±15% could be expected over a ±5°C span. In the receiver circuit this would cause by far the largest temperature related effect. The detector spectral response is that of a silicon detector. The spectral effects are discussed in Section 7.

6.0 SOURCE

The source used was an 1815 type tungsten lamp which is a 14 V 0.20A 1.4 candela lamp with a C-2V filament with a T 3 bulb size and a nominal 3000 hr lifetime. No filament sizes are given in

manufacturer's data. Using Spectro's catalogue 10/82 and the curve on p 5 of this catalogue and the fact that the candela to electrical power ratio is 0.5, one can estimate that the color temperature of the source is approximately 2400 K.

The lamp power variation is determined by the voltage regulator stability. The lamp regulator provides "typical" regulation of line and load of 0.23% and worse regulation of 2.7%. The radiant emittance of the lamp is proportional to the 3.5 power of the input voltage so that for small variations the emittance variation is 3.5 x the voltage regulation. Thus a typical emittance regulation of 0.8% and a worst case regulation of 9.5% may be expected.

The temperature regulation of the regulator is typically 0.007%°C. This yields a variation of 0.035% in the voltage and 0.12% in the lamp output over ±5°C.

7.0 SPECTRAL RESPONSE

The existing instrument's spectral response is essentially determined by the combination of the source spectral output and the detector spectral responsivity. The fiber spectral response is essentially uniform over the spectral region of interest and may be neglected. One may also neglect to the first order the spectral response of the water.

The detector used is a silicon detector. The nominal spectral response used was given in the sensor manufacturer's data sheet.

The tungsten source spectral response figure was estimated using the spectral radiance of 2400 K blackbody. The spectral emittance of tungsten is approximately uniform over the spectral region of interest and was not included. The source and detector

responses were combined and normalized to give the system relative spectral response. The results show that the response is peaked at 900 nm and is skewed in the red (see Figure 13).

For reduced sensitivity of the instrument to varying soil bottom conditions it would be desirable, in general, to select a region of response where the soil reflectivity is spectrally flat. Examination of the spectral reflectivities of various soils (taken from G.H. Suits, "Natural Sources" in The Infrared Handbook, W. Wolfe and G. Zissis, eds., Environmental Research Institute of Michigan, Ann Arbor, pp 3-86 to 3-88), indicates that for most soils the spectral reflectivity is essentially flat between 600 and 1000 nm. Thus the spectral response of the detector/source combination is probably as good as can be expected for this particular consideration.

The ambient light effects were likely caused by radiation from 300 to 680 nm which both fluorescent and metal halide sources emit. If a red filter is introduced to essentially reduce to zero this radiation, the effects of ambient fluorescent or metal halide lamps should be greatly reduced. The experimental results confirmed this. Tungsten incandescent sources peak in the near infrared. Since the sensor source is itself of this type, simple filtration of ambient incandescent type illumination would be ineffective.

8.0 CONDUCTOR TRACES

The cable conductors are assumed to be #24 AWG which would give a resistance of approximately 20 mΩ/foot. (This is also equivalent to a PCB track 0.2" wide made from one ounce copper board).

Current/voltage drops due to ground "dispersion" are likely not serious at low frequencies.

Drive voltages due to the servo may affect signal levels. The degree of coupling is best determined experimentally. About 60db or greater isolation is required to ensure that the millivolt level pre-amp signals are not affected by the volt level servo inputs.

9.0 THE EFFECT OF SUSPENDED MATERIAL ON THE SENSOR

Consider a very simplified model of the sensor as shown

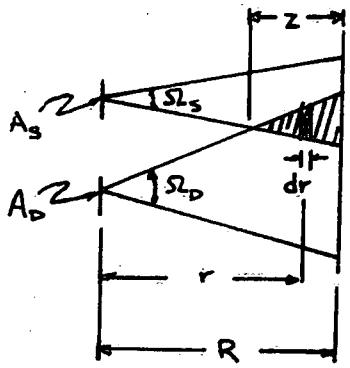

where
- A_S = area of the source
- A_D = area of the detector
- R = distance of the bottom from the source/detector plane
- r = distance from the source/detector plane to an elemental slice of thickness dr.
- z = distance from intersection point of source and detector fields to the bottom or target
- L_S = source radiance
- ρ = bottom diffuse reflectance
- Ω_S = source emission solid angle
- Ω_D = detector acceptance solid angle

For simplicity consider that the source illuminated area is larger than the area sensed by the receiver. This is not strictly correct, since it is precisely the reason why the reduction in signal occurs when the target, i.e., bottom is very close to the source/detector plane. If we consider the target to move toward the probe tip, after the probe passes the distance z in the attached figure, no intersection volume is left and hence the reduction of signal occurs. For the situation of interest, however, where the probe is sufficiently far away the approximation should be reasonably valid. A nearly exact formulation exists which has determined the intersection volume reasonably precisely (S.K. Pal, York University, under contract to DOE). However, the order of magnitude of the effect is of more interest in this present case and thus the simpler analysis is used.

In the the case of light scattered and absored, the normal representation is to consider the attenuation of light, with the attenuation coefficient as the sum of the absorption coefficient a and the scattering coefficient s., i.e., $\alpha = a + s$. This, however, is inadequate in the present instance since, for large particles especially, a large fraction of the scattered light is in the forward direction. Thus light scattered by a single particle is re-directed into the beam. Thus the attenuation coefficient including this re-directed radiation which is called γ is used (see W. Wells, "Factors Affecting Long Range Vision" in Optics of the Sea, Agard Lecture Series No. 61, NATO, 1973, p 4.1.4).

As a rule of thumb, in a 20° cone (the precise angle is not important)

$$\gamma = a + \int_{10^\circ}^{\theta_{max}} \sigma \, dw$$

where σ is the volume scattering function, and dw is the elemental solid angle.

From elementary considerations, the differential power $d\phi$ to the target is given by

$$d^2\Phi = L_S \, d\underline{\Omega}_S \, \underline{n} \cdot d\underline{A}_S$$

where $d\Omega_S$ = elemental solid angle of the source
$\underline{n}$ = a unit vector perpendicular to the direction of propagation.
$d\underline{A}_S$ = the source area vector.

Assuming uniformity one may substitute the integral values. Thus, $\Phi = L_S \, \Omega_S \, A_S$ is the power incident on the target. (Neglect non-normal effects which are small).

The irradiance E on the target of area A_T is $E = \frac{\Phi}{A_T}$.

The radiance of the target, assuming a diffuse reflectance ρ is simply $L_T = \rho \frac{E}{\pi}$ since π is the projected solid angle. But $A_T = \Omega_S R^2$.

Thus $L_T = \frac{\rho}{\pi} \frac{L_S \Omega_S A_S}{\Omega_S R^2}$.

The power at the detector is by similar considerations

$$\Phi_D = L_T \, \Omega_D A_D = \frac{\rho}{\pi} \frac{L_S A_S A_D}{R^2}$$

Including attenuation $\Phi_{DT} = \frac{\rho}{\pi} \frac{L_S A_S A_D}{R^2} e^{-2\gamma R}$, because of the round trip distance 2R.

Similarly, the return from the water elemental slice dr is

$$d\Phi_w = \sigma_b \frac{L_S A_S A_D}{R^2} e^{-2\gamma/r} dr. \qquad (2)$$

The factor π is not included since this is included in σ. A single σ_b, i.e., backscattered volume scattering function is used since angular effects in the backscattering are small. Neglect L_S, A_s and A_D since these are common terms between equations (1) and (2). This gives

$$\phi_{DT} = \frac{\rho}{\pi R^2} e^{-2\gamma r}$$

The integral of the last equation must be evaluated. Namely

$$\phi_w = \sigma_b \int_{R-2}^{R} e^{-2\gamma r} \frac{dr}{r^2}$$

For simplicity set $r = R-z$, except in the exponent, which gives the most important limiting value of r. (The actual integral is tabulated but the resultant improvement in accuracy is not warranted here since only approximate values are desired.)

Thus $$\phi = \frac{\sigma_b}{(R-z)^2} \int_{R-z}^{R} e^{-2\gamma r} dr$$

$$= \frac{\sigma_b}{(-2\gamma)(R-z)^2} [e^{-2\gamma R} - e^{-2\gamma(R-Z)}]$$

$$\phi_{DW} = \frac{\sigma_b}{2\gamma(R-Z)^2} e^{+2\gamma z}$$

Assume that $\phi_{DW} < 0.25\ \phi_{Dr}$, i.e., the backscattered radiation from the suspended material is 25% of the reflected radiation from the bottom for adequate detection.

Suppose $R/Z = 3$

Use San Diego Harbour data (similar to normal Lake Ontario water) and normalize it to obtain the normalized volume scattering function, and to determine γ.

Using Scripps data for station 2040 (San Diego Harbour) $\sigma = 2.2\ m^{-1}$, $s = 1.8$, $a = 0.4$. The value of $s\int_{10°}^{180°} \sigma\, dw \simeq 0.34\ s = 0.61$. Thus $\gamma \simeq 1\ m^{-1}$, $\sigma_b \simeq 10^{-2} m^{-1}$

Suppose $\rho \simeq 0.2$

and $z = 3\ mm = 0.003\ m$, $R = 9\ mm = 0.009\ m$. The exponent is nearly unity

Thus $$\phi_{DW} = \frac{10^{-2}}{2(0.006)^2} = 1.38 \times 10^2$$

$$\phi_{DT} = \frac{0.2}{\pi(0.009)^2} = 7.8 \times 10^2$$

Thus $\phi_{DW} \simeq 0.2\ \phi_{DT}$ which should be okay.

For larger attenuation coefficients no data is available in the literature and it would be pure conjecture to estimate the effect.

10.0 BOTTOM REFLECTANCE VARIATIONS

Three curves from a tabulation of several dozen spectal reflectance curves from the article by G.H. Suits referenced in Section 7 are reproduced here. See Figures 14 through 16. It is apparent that factors of five are possible in natural conditions confirming the measurements discussed in Section 3. Smaller variations occur within soils of the same class.

11.0 SUMMARY OF THE SENSITIVITY OF THE SENSOR TO VARIOUS CAUSES AS CALCULATED

Item	Typ.	Max.	Remedial action
1) Target reflectance	factor of 4	>factor of 10	nil with this sensor type, apart from normal calibration for each bottom.
2) Temperature			
(a) sensor		±15% over ±5°C	use improved detector, filter radiation beyond 950 nm
(b) pre-amp resistors		±500 ppm over ±5°C	not required.
(c) amplifier resistors		0.12% over ±5°C	not required.
(d) pre-amp input		±9 mV over ±5°C typ. referred to output	not required.

(e) amp. input offset voltage variation	±500 μV over ±5°C typ. referred to output	not required.
(f) input bias current of preamp.	negligible	not required.
(g) input bias current of pre-amp	negligible	not required.
(h) source regulator (x6 for effect on illuminance)	±0.12% over ±5°C on illuminance	not required.

3) Time

(a) sensor	unknown but likely small	
(b) source (due to line & load regulatory variations)	10% max, 1% typ	Improved regulator for adjustment. Change offset adjustment to final stage.
(c) time drift of opamps	not specified but likely relatively small	
(d) variations in offset voltage adjustment circuitry due to regulator variation	70 mV	Better regulation for adjustment. Change offset adjustment to final stage.

4) Noise	Typ.	Worstcase	Possible Remedial Action
(a) sensor	1.3 mV	13 mV	better photo-detectors
(b) amplifiers	<100 µV		not required
(c) resistors			not required
(d) circuit/ cables/cross sampling	unknown		reduce bandwidth

5. Ambient Light

sensor	±2mm sensitivity in linear region (measured) typical	1. Use red filter such as Corning 2-64 or Rosco #823.

6. Bandwidth

Bandwidth of sensor >10KHz which is excessive. Reduce to 1 KHz by increasing feedback capacitors.

11 ALTERNATIVE SENSORS

The fundamental limitation of the fiber optic probe type in its use as a flume profiler is that it is dependent upon measurement of the light value reflected from the bottom. It is thus inherently sensitive to variations in the reflectivity characteristics of the bottom. Thus even assuming ideally stable detectors and sources the sensor output may easily vary by a factor of four depending upon whether the bottom type would be, for instance, sand of quartz and rock fragments or clay (see G.H. Suits previously referenced).

I have proposed a sensor type which would substantially reduce and perhaps essentially eliminate the effects of bottom reflectivity. The essential characteristics are as follows: A collimated light source (e.g., a laser) illuminates the bottom at an oblique angle θ from the normal to the bottom. A receiver consisting of a lens and a position sensitive detector is mounted adjacent to the source. If the bottom height is changed from position 1 to position 2 the spot on the bottom illuminated by the source is changed a horizontal distance. This distance is imaged onto the position sensitive receiver at a distance from the optical axis y' where $y' = my$, with m being the magnification. The transverse distance y is related to the longitudinal height change l by $y = l \tan \theta$ and $y' = mL \tan \theta$. Thus a height change l is measured by measuring a transverse distance in an image plane. There are a large number of position sensitive detectors, e.g., vidicon camera charge coupled arrays, photo diode arrays, quadrant detectors, etc. Perhaps the simplest is a position sensitive photodiode manufactured by Silicon Detector Corporation and United Detector Corporation. In this device, as the beam is incident on the detector, photoelectrons are generated. The relative amount of photoelectrons sensed by the "bridge arm" A

compared to the "arm" B is a function of the beam spot (or centroid) position. The position is a function of the relative photocurrents generated, i.e., $y' = k(A-B)/(A+B)$. Two axis detectors or single axis detectors may be obtained. The photocurrents are easily calculated using a microcontroller or desk top computer.

The advantage of this kind of detector is that the absolute magnitude of the incident beam is not required as long as it falls within the detector noise and saturation limits. Thus variations due to source fluctuations, bottom reflectivity, etc., are relatively unimportant. Moreover, no servo system is required since the output "error" is directly given.

The linearity of the detector is dependent upon the linearity of the photodetector itself (which is excellent) and the linearity of the magnification. This is only linear where l is a small fraction of L. In principle this may be compensated for by an initial calibration.

Secondly, the absolute accuracy of the system is governed by the accuracy of the photodetector. The photodetector absolute accuracies are only ±0.1 mm, but have resolution to nanometres. The accuracy figures are because of non-linearities. These again, however, may be corrected by calibration. Temperature effects of the photodetector are typically ±1μm/°C. Thus over ±10°C operation resolutions of ±10μm in the detector plane are possible. If $\theta = 10°$ say, and $m \approx 0.05$ (50 mm lens, $L \sim 1$m), then the variations in l that can be resolved are

$$l \sim \frac{\pm 10\ \mu m}{(0.05)(\tan 10°)} = \pm 1\ mm.$$

The above analysis should in no way be considered a detailed design. Noise and signal level considerations may render the concept invalid.

13.0 RECOMMENDATIONS

1. Sensor performance is limited by the sensitivity of the sensor to target (bottom) reflectance. This is inherent in the design of the fiber optic probe. The only relatively easy way to correct this is through an operational procedure - namely, perform a sensor output vs distance from the probe calibration, and then recursively adjust the sensor gain and offset until a normalized curve is achieved, so that the servo receives a set voltage vs distance signal.

   This would require the addition of some micrometer stage attachment to the sensor head mount to enable these adjustments. Additionally the adjustment potentiometers would likely have to be mounted to the front panel, or access holes to circuit board mounted potentiometers would have to be provided. Whether or not such a process is acceptable can only be answered by the users. If it is not, then a new sensor type is required.

2. Ambient light effects are present, but are not of the same order of magnitude as the bottom reflectance effect. Under typical (500 lux) discharge lamp ambient illumination conditions, the effects can be substantially reduced by incorporating a red filter such as a Corning 2-64 between the receiver and detector. This should be very easy to do.

3. Source regulation is relatively poor. This may be corrected by improving the lamp regulator. A re-designed regulator would be required.

4. Detector temperature response is poor. This may be corrected by using a better sensor such as an EG&G UV-100A. Some mechanical modifications would be required. This would also require

reconfiguring the pre-amp as a current to voltage converter, this would in the process remove two resistors and increase the value of one. Also the radiator beyond 950 nm should be removed for reduced temperature response. This latter item however would require a special filter and would be expensive.

5. Offset voltage reference voltages should have improved regulation. If the existing three stages of amplification are still desired, the offset voltage adjustment should be moved to the last stage to reduce multiplication effects.

6. It should be noted that the existing offset voltage circuitry will not allow large (±5V) offsets to adjust the offset to allow sensor "zero" position in the position of maximum linearity. It is not certain whether this would be allowed by the variation of existing potentiometers in the servo portion of the circuit (amplifiers four and subsequent) since analysis of the servo circuit was outside of the author's mandate. The adjustment range could be extended however by changing component values.

7. Sensor workmanship was noted to be poor. Solder flux was not cleaned, mechanical mountings were marginal, various grounds were distributed over the sensor card. The extent of the contribution of poor workmanship to sensor innaccuracies is not fully known. It is not expected that these effects would exceed the effect of target reflectance or sensor noise. Distributed grounds would have less of an impact than improper cabling because of the relatively longer length of the latter. It is recommended that some rework be done, if only to improve the maintainability of the device and to improve confidence in its operation. It is understood that re-work of the interface cable is already underway. The new cable should be checked to ensure that isolation between sensor and servo signals be between 50 and 60 db.

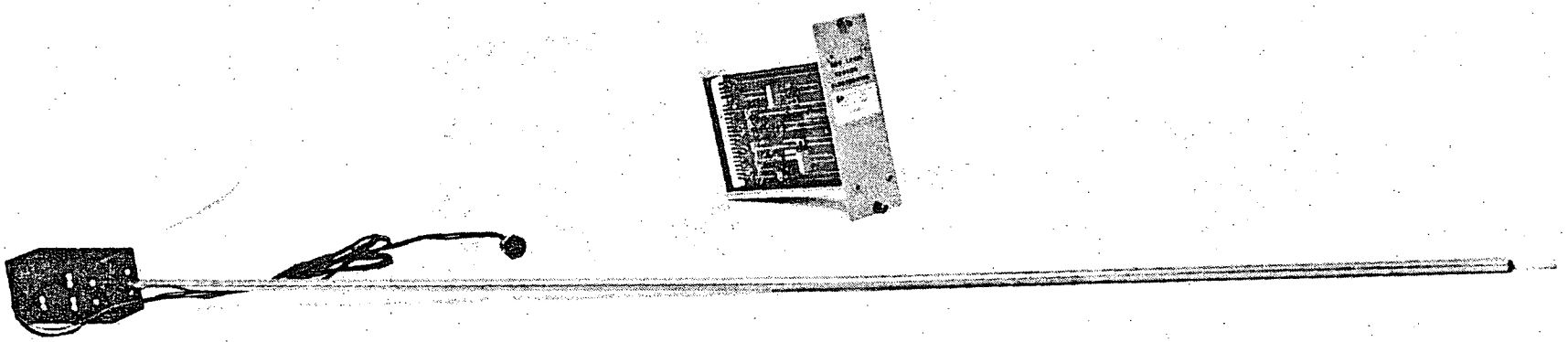

FIGURE 1. Photoview of Bed-Level Sensor: Probe-plus-Electronics.

FLUME PROFILER SERVO ERROR–IDEALIZED RESPONSE

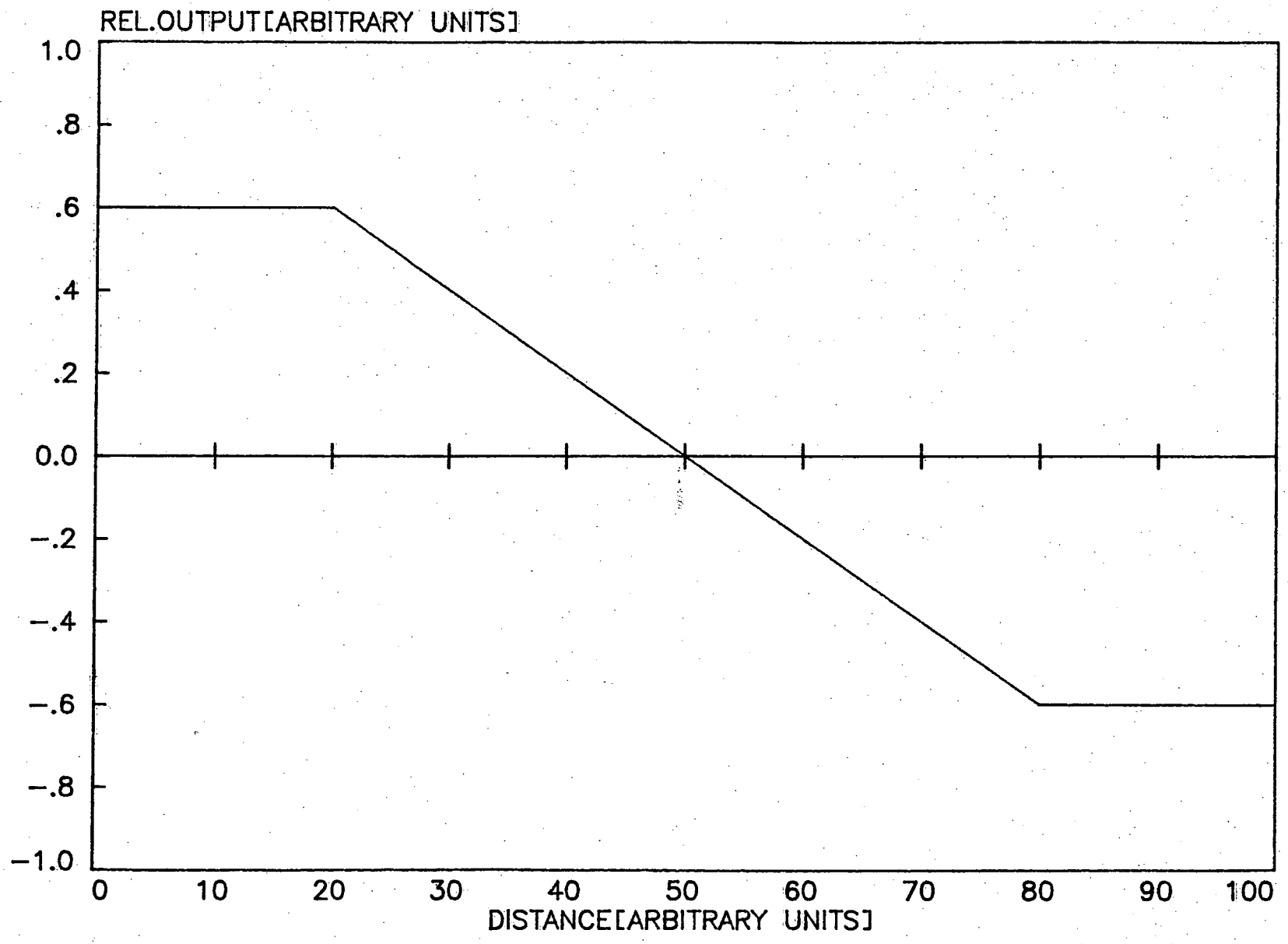

FIGURE 2.

FIGURE 3.

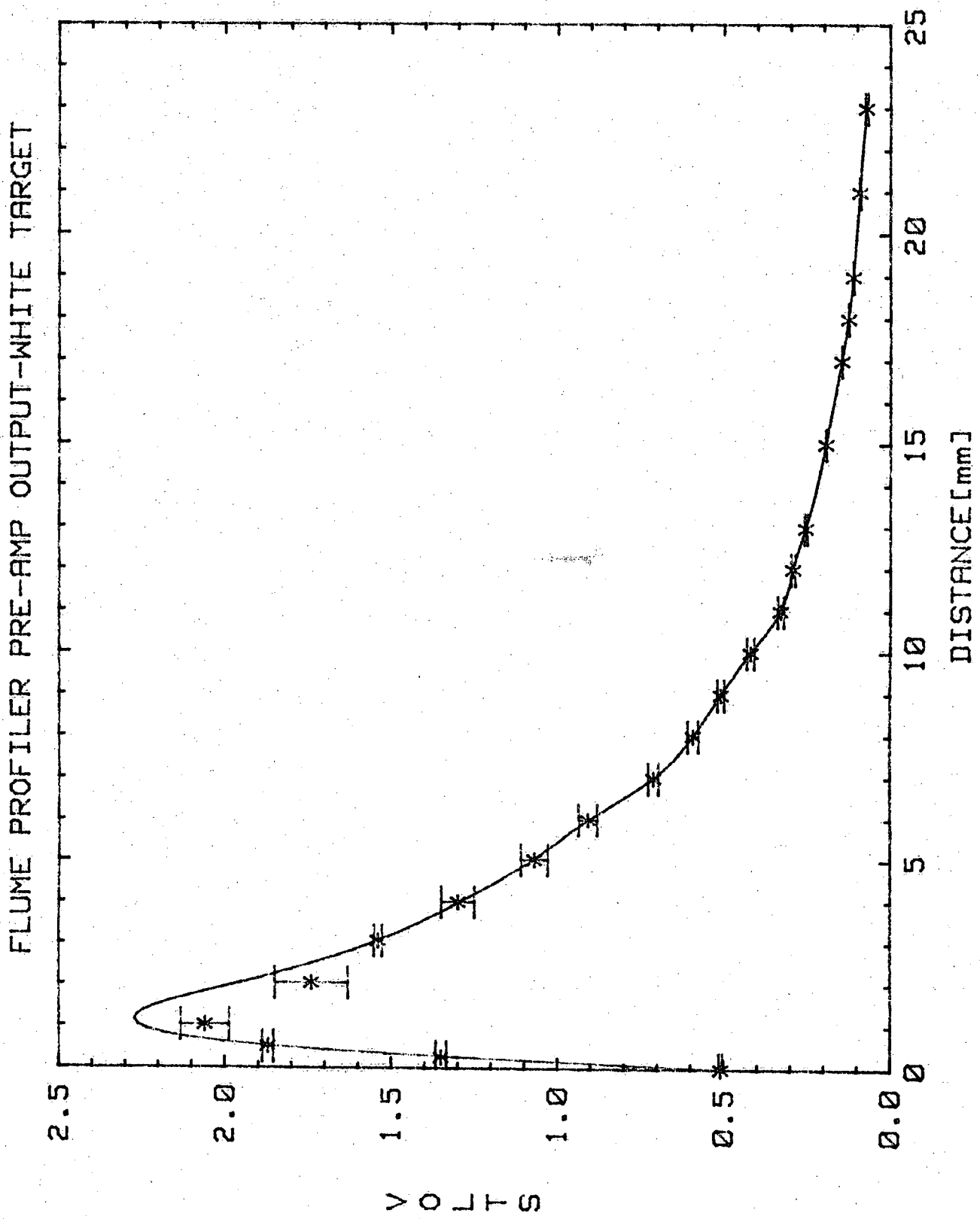
FLUME PROFILER PRE-AMP OUTPUT-WHITE TARGET
VOLTS
2.5
2.0
1.5
1.0
0.5
0.0
0
5
10
15
20
25
DISTANCE[mm]

FIGURE 4.

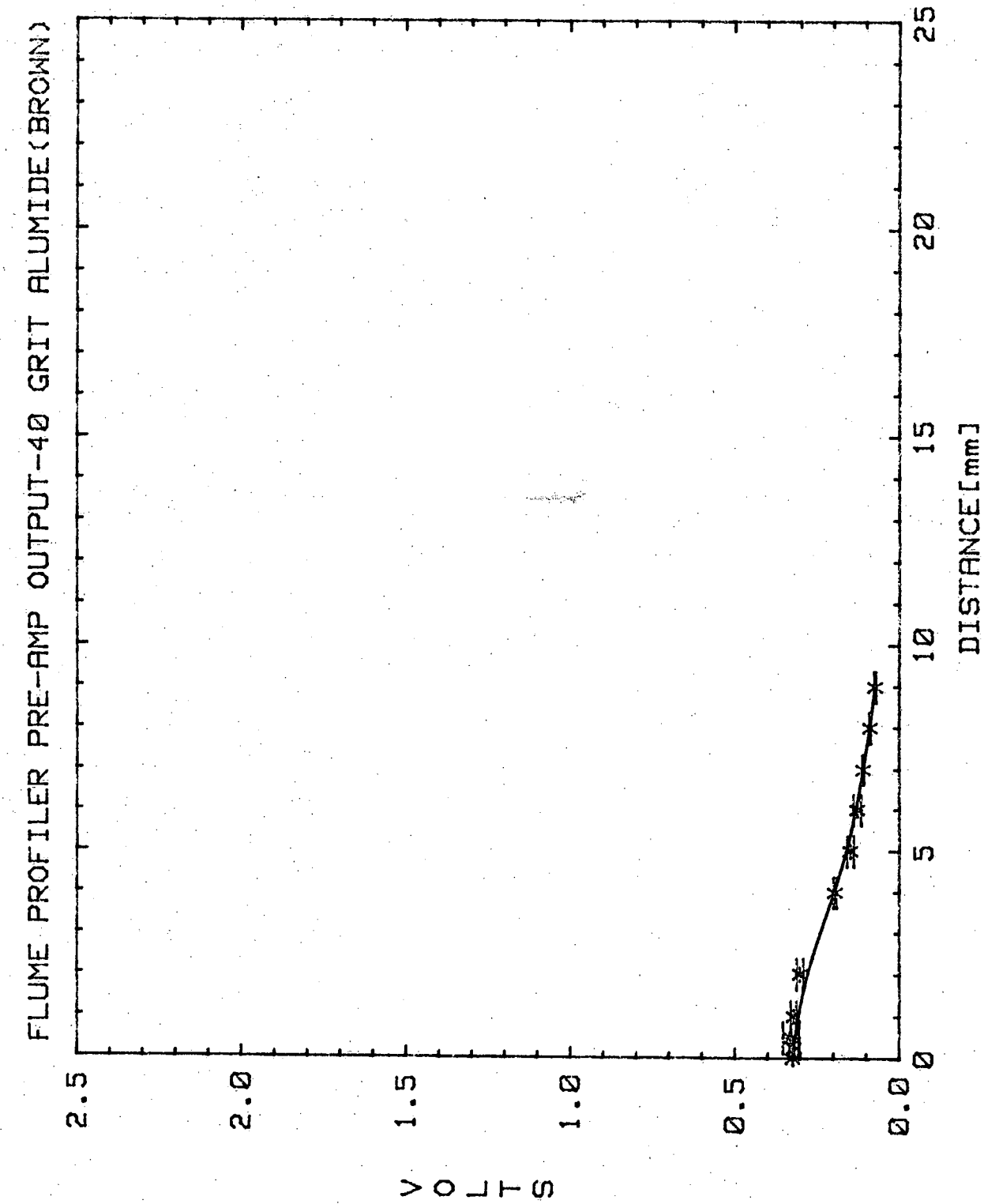
FLUME PROFILER PRE-AMP OUTPUT-40 GRIT ALUMIDE(BROWN)
VOLTS
2.5
2.0
1.5
1.0
0.5
0.0
0
5
10
15
20
25
DISTANCE[mm]

FIGURE 5.

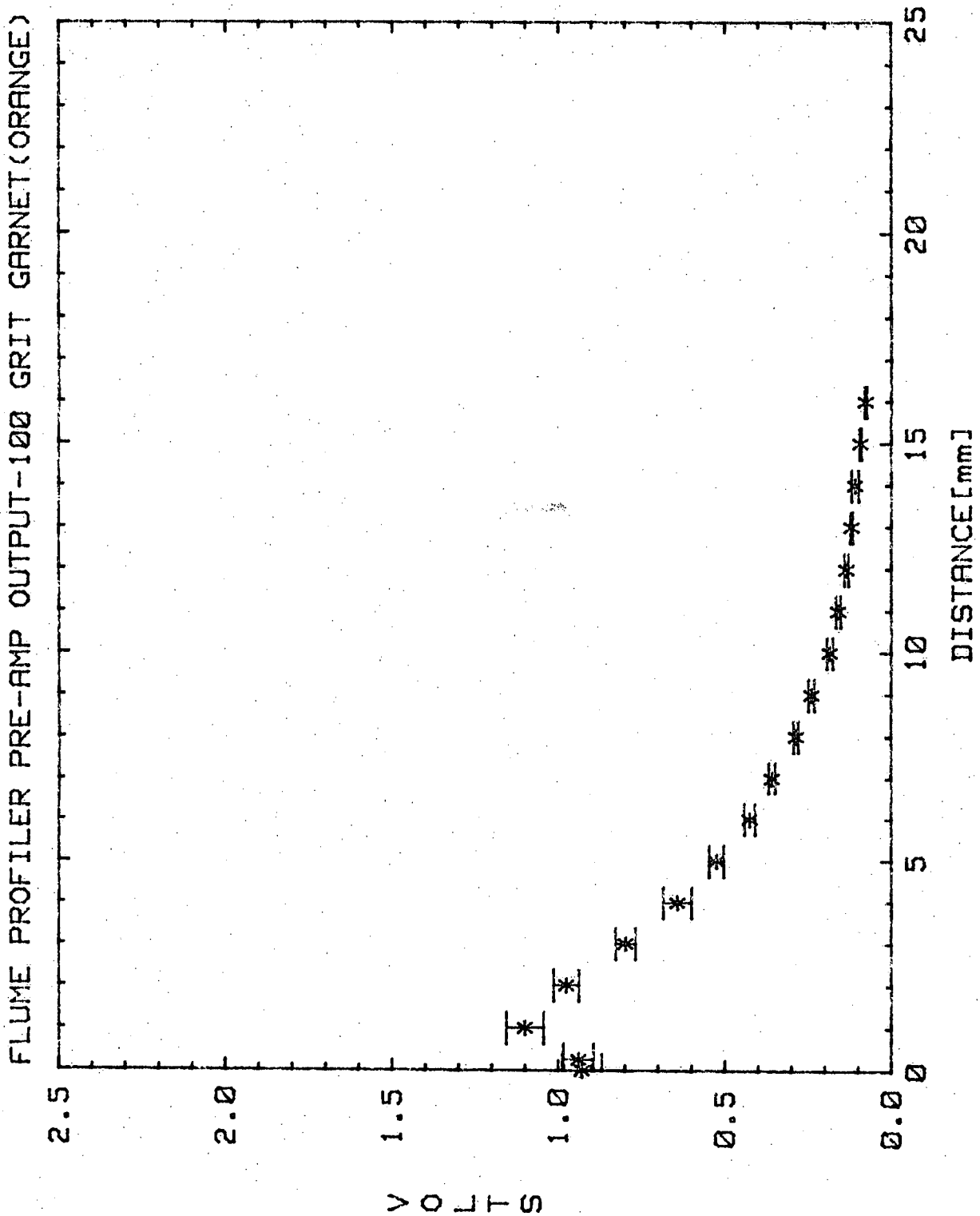
FLUME PROFILER PRE-AMP OUTPUT-100 GRIT GARNET(ORANGE)
VOLTS
2.5
2.0
1.5
1.0
0.5
0.0
0
5
10
15
20
25
DISTANCE[mm]

FIGURE 6.

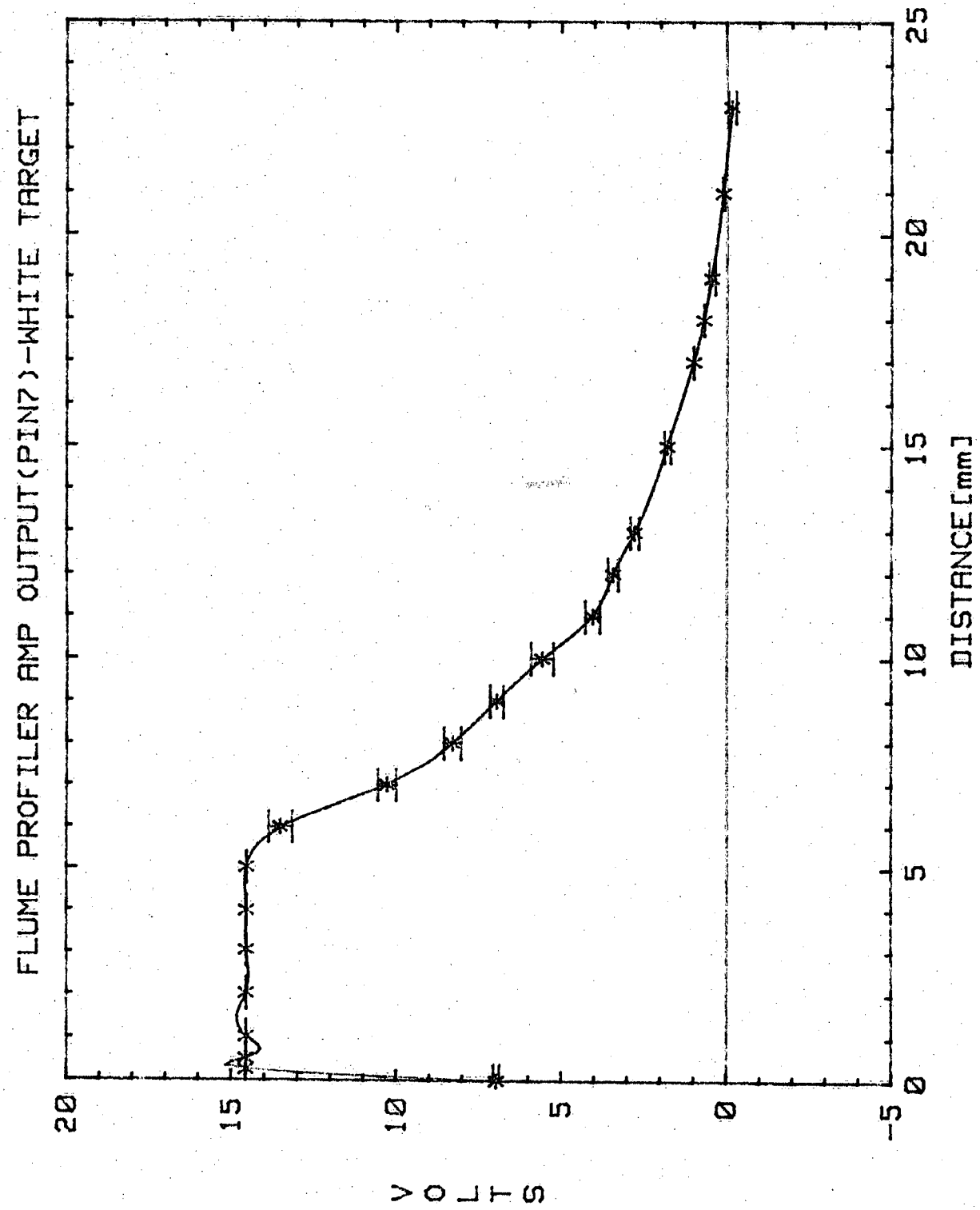
FLUME PROFILER AMP OUTPUT(PIN7)-WHITE TARGET
VOLTS
20
15
10
5
0
-5
0
5
10
15
20
25
DISTANCE[mm]

FIGURE 7.

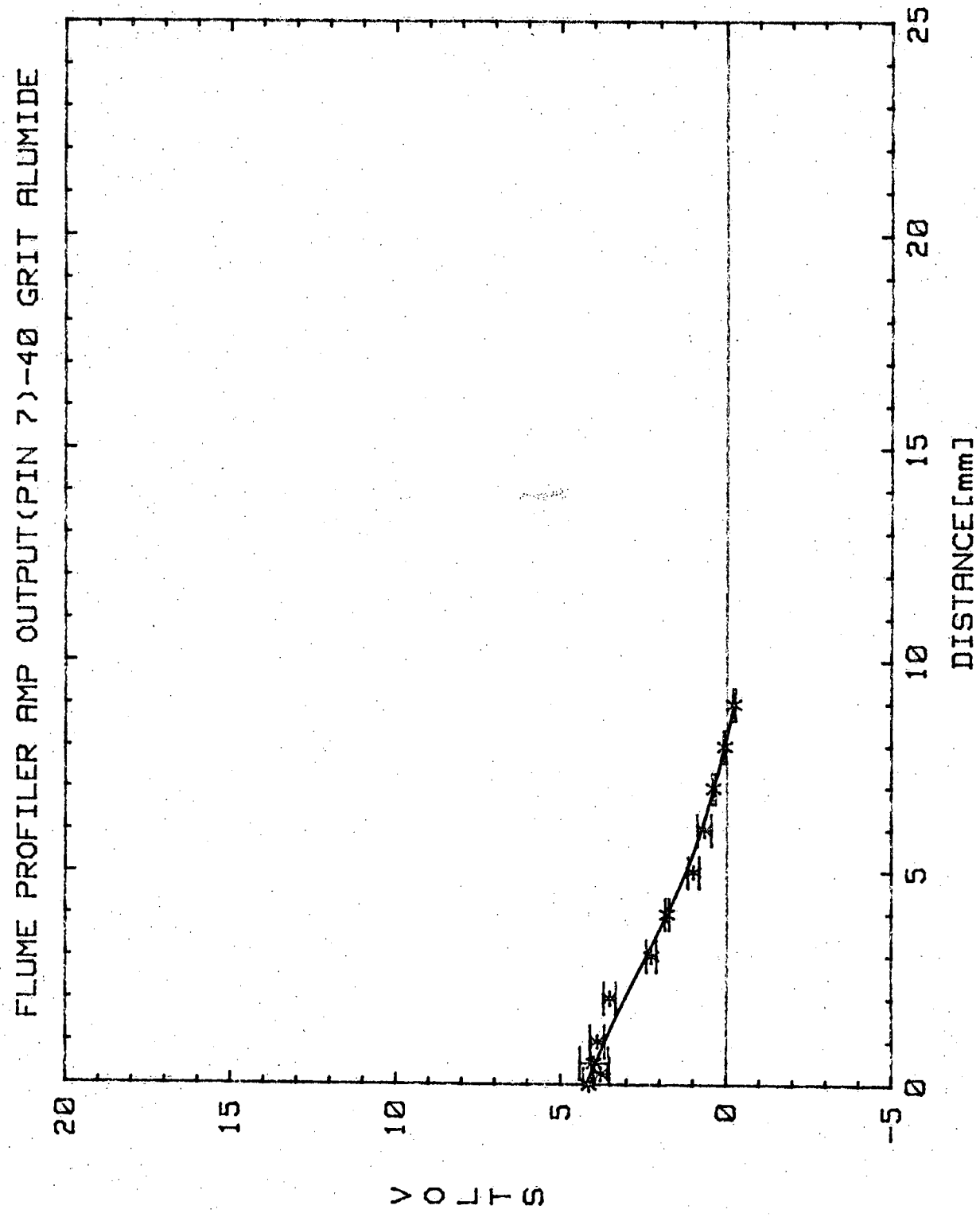
FLUME PROFILER AMP OUTPUT(PIN 7)-40 GRIT ALUMIDE
VOLTS
20
15
10
5
0
-5
0
5
10
15
20
25
DISTANCE[mm]

FIGURE 8.

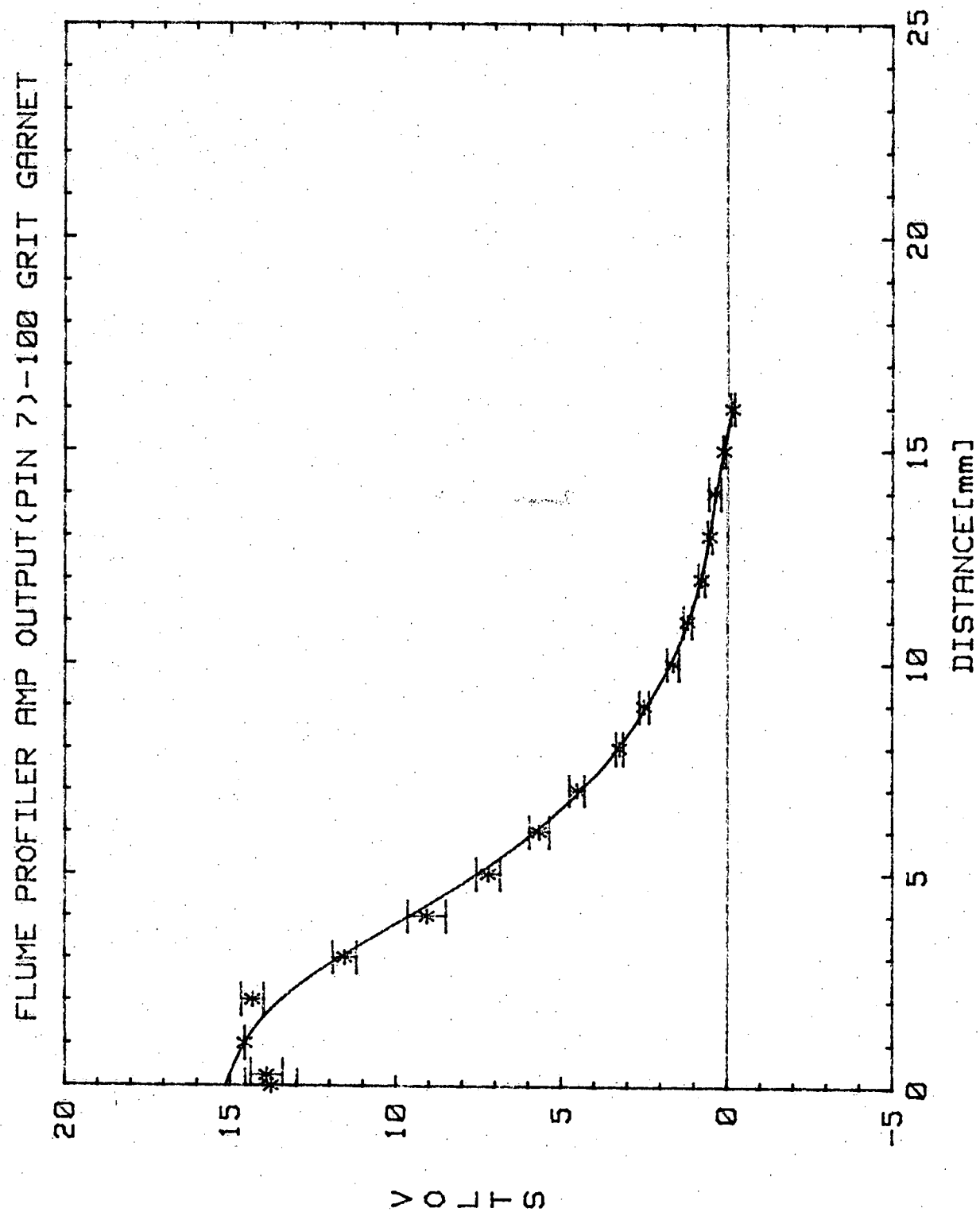
FLUME PROFILER AMP OUTPUT(PIN 7)-100 GRIT GARNET
VOLTS
20
15
10
5
0
-5
0
5
10
15
20
25
DISTANCE[mm]

FIGURE 9.

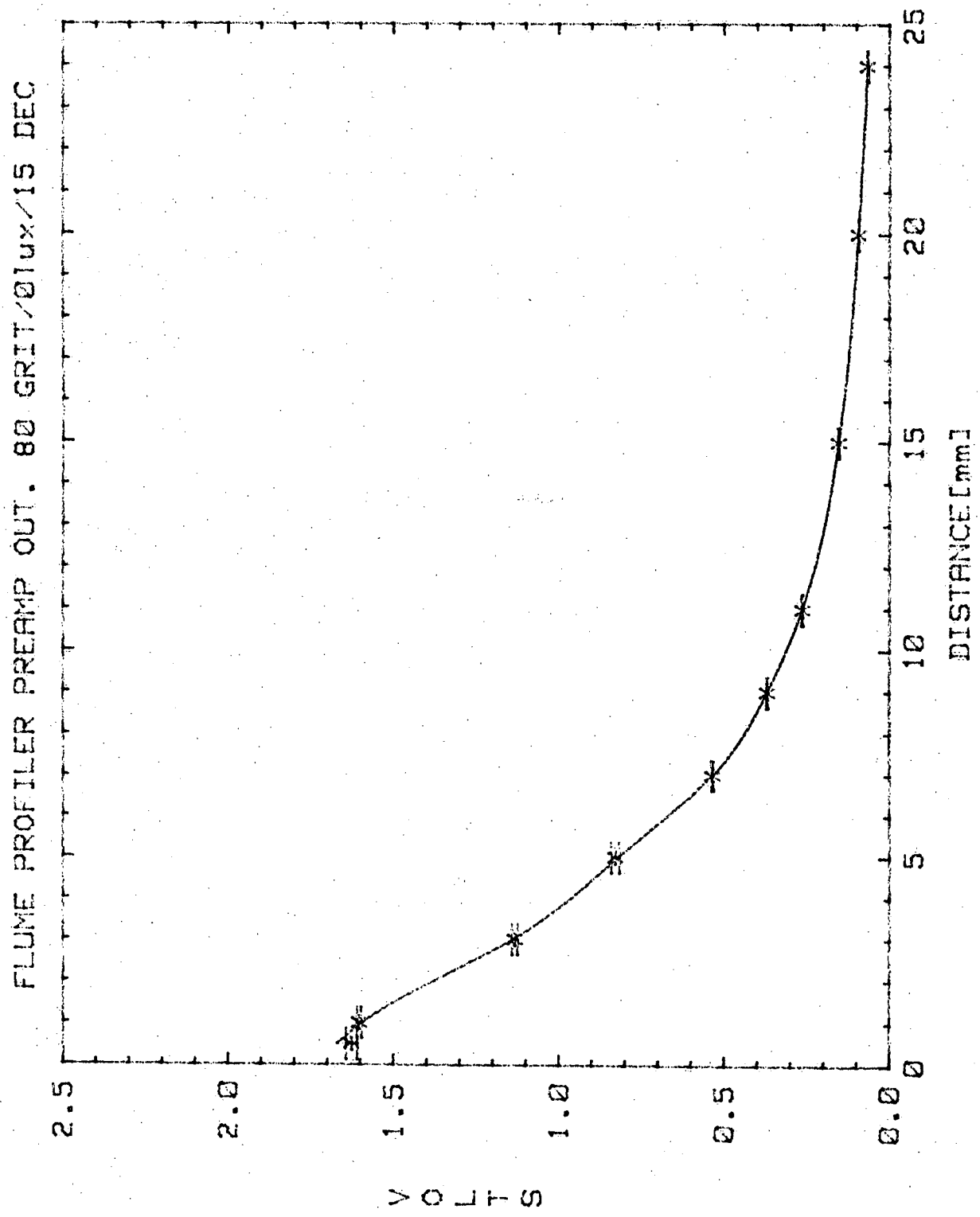
FLUME PROFILER PREAMP OUT. 80 GRIT/01ux/15 DEC
VOLTS
2.5
2.0
1.5
1.0
0.5
0.0
0
5
10
15
20
25
DISTANCE[mm]

FIGURE 10.

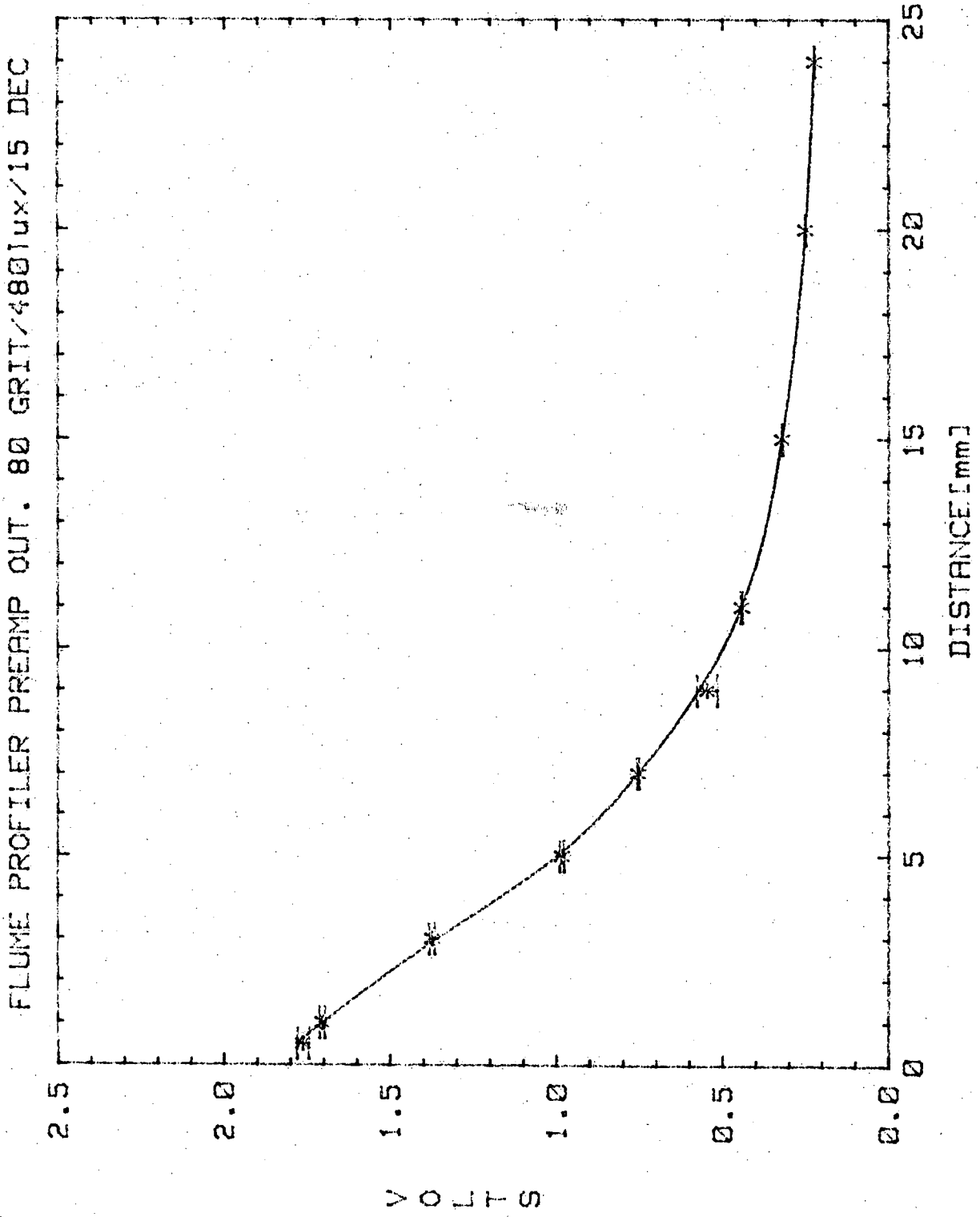
FLUME PROFILER PREAMP OUT. 80 GRIT/480lux/15 DEC
SIGNAL
2.5
2.0
1.5
1.0
0.5
0.0
0
5
10
15
20
25
DISTANCE[mm]

FIGURE 11.

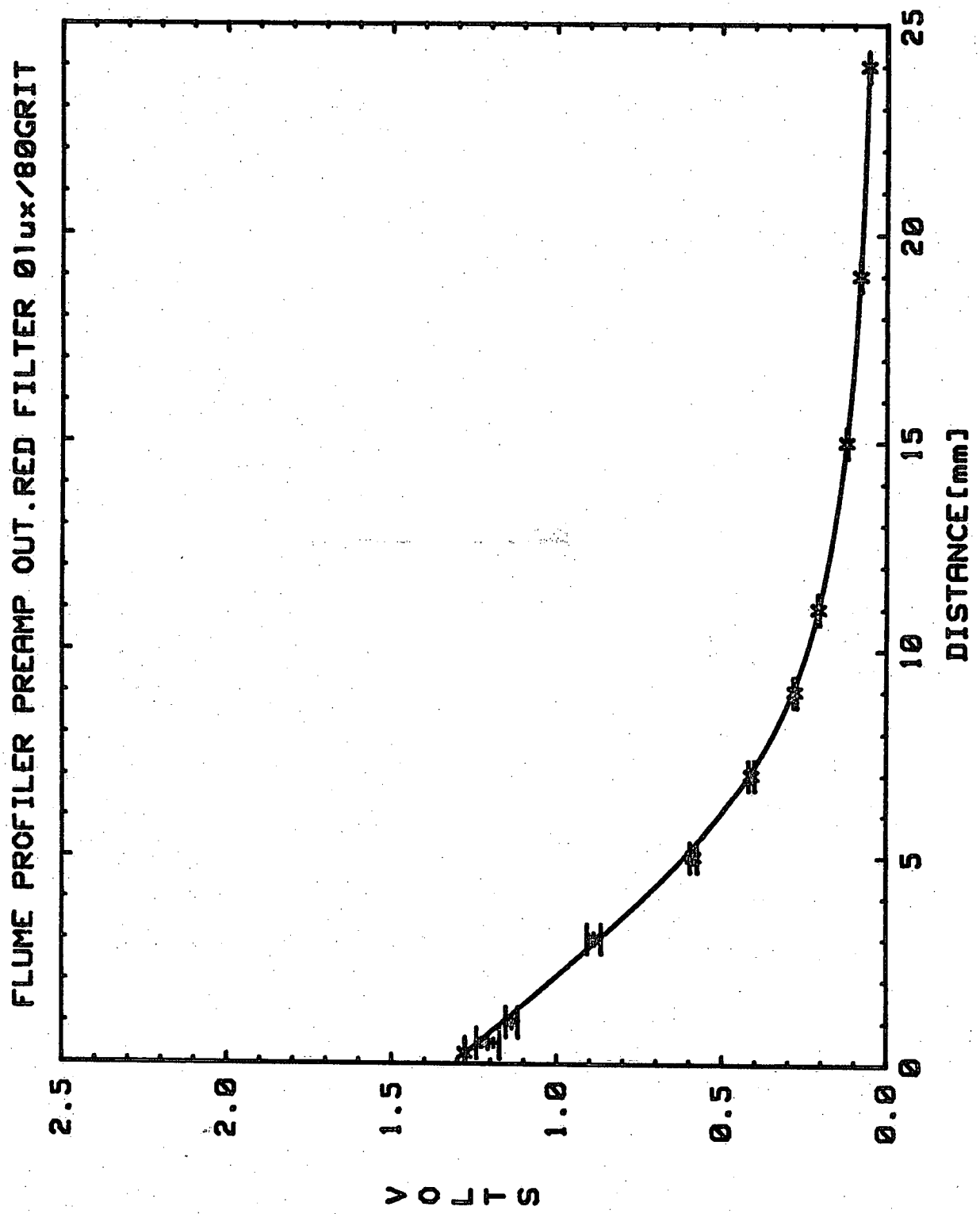
FLUME PROFILER PREAMP OUT.RED FILTER 01ux/80GRIT
VOLTS
2.5
2.0
1.5
1.0
0.5
0.0
0
5
10
15
20
25
DISTANCE[mm]

FIGURE 12.

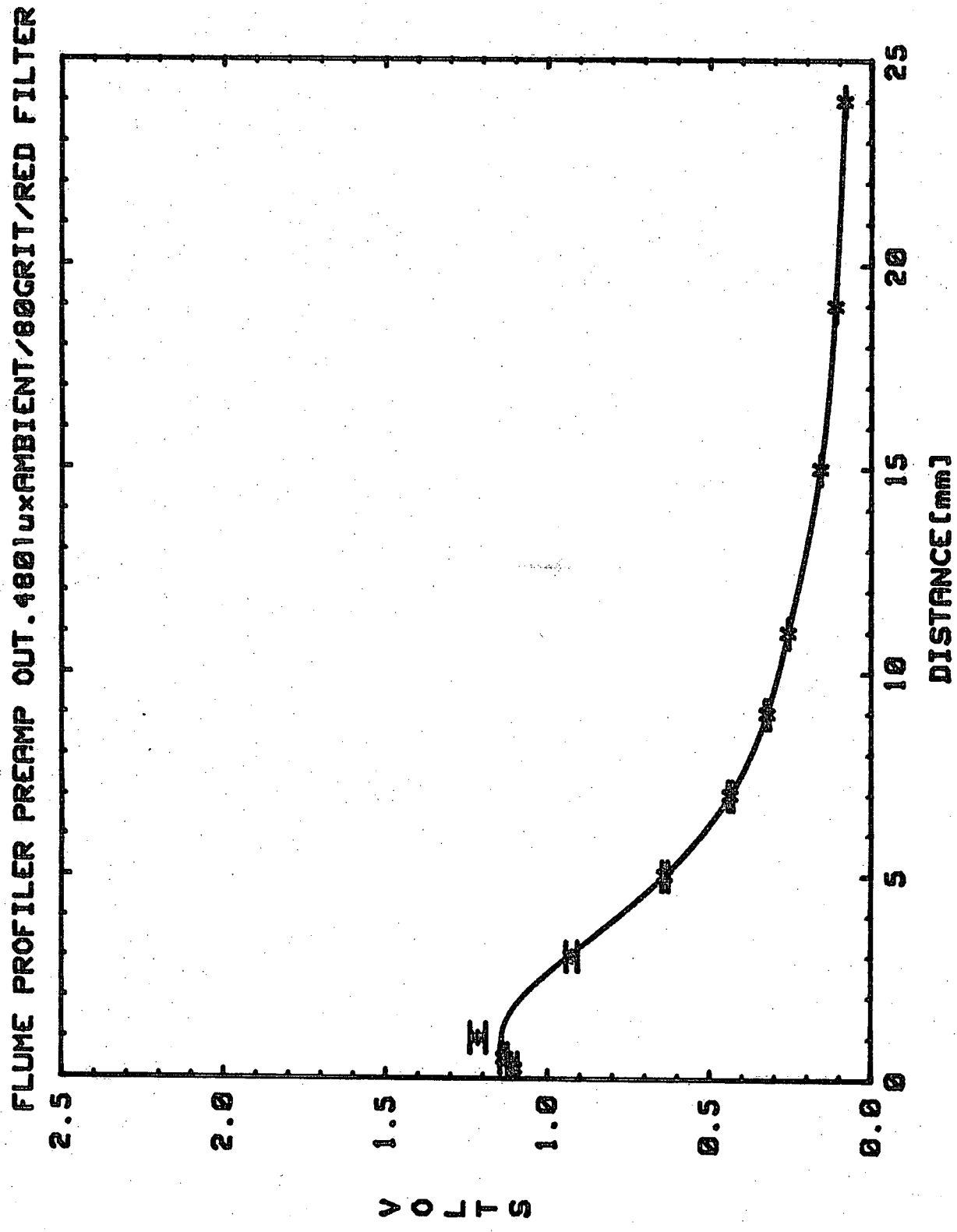
FLUME PROFILER PREAMP OUT.480luxAMBIENT/80GRIT/RED FILTER
VOLTS
2.5
2.0
1.5
1.0
0.5
0.0
0
5
10
15
20
25
DISTANCE[mm]

FIGURE 13.

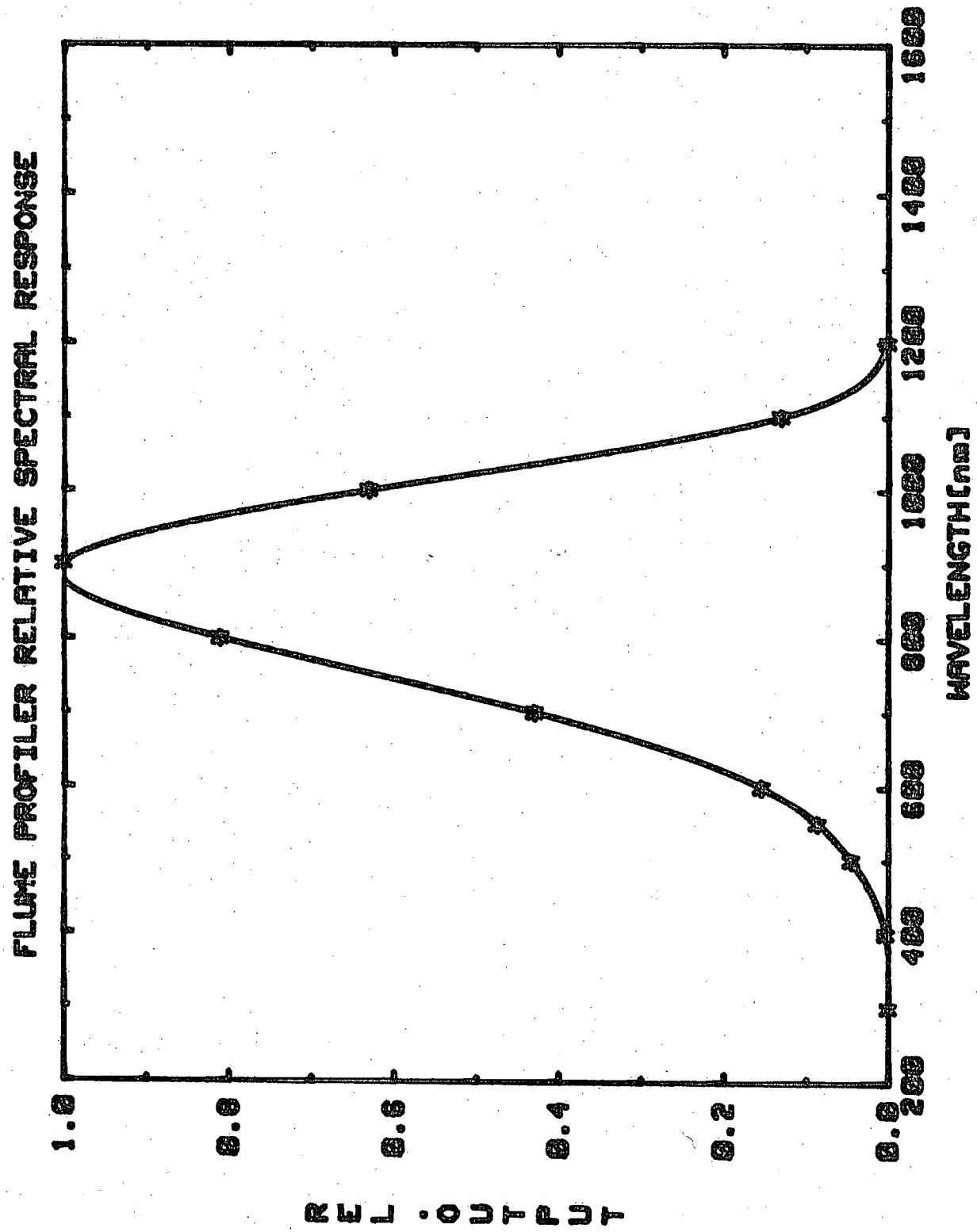
FLUME PROFILER RELATIVE SPECTRAL RESPONSE
1.0
0.8
0.6
0.4
0.2
0.0
200
400
600
800
1000
1200
1400
1600
WAVELENGTH[nm]
RELATIVE OUTPUT

FIGURE 14.

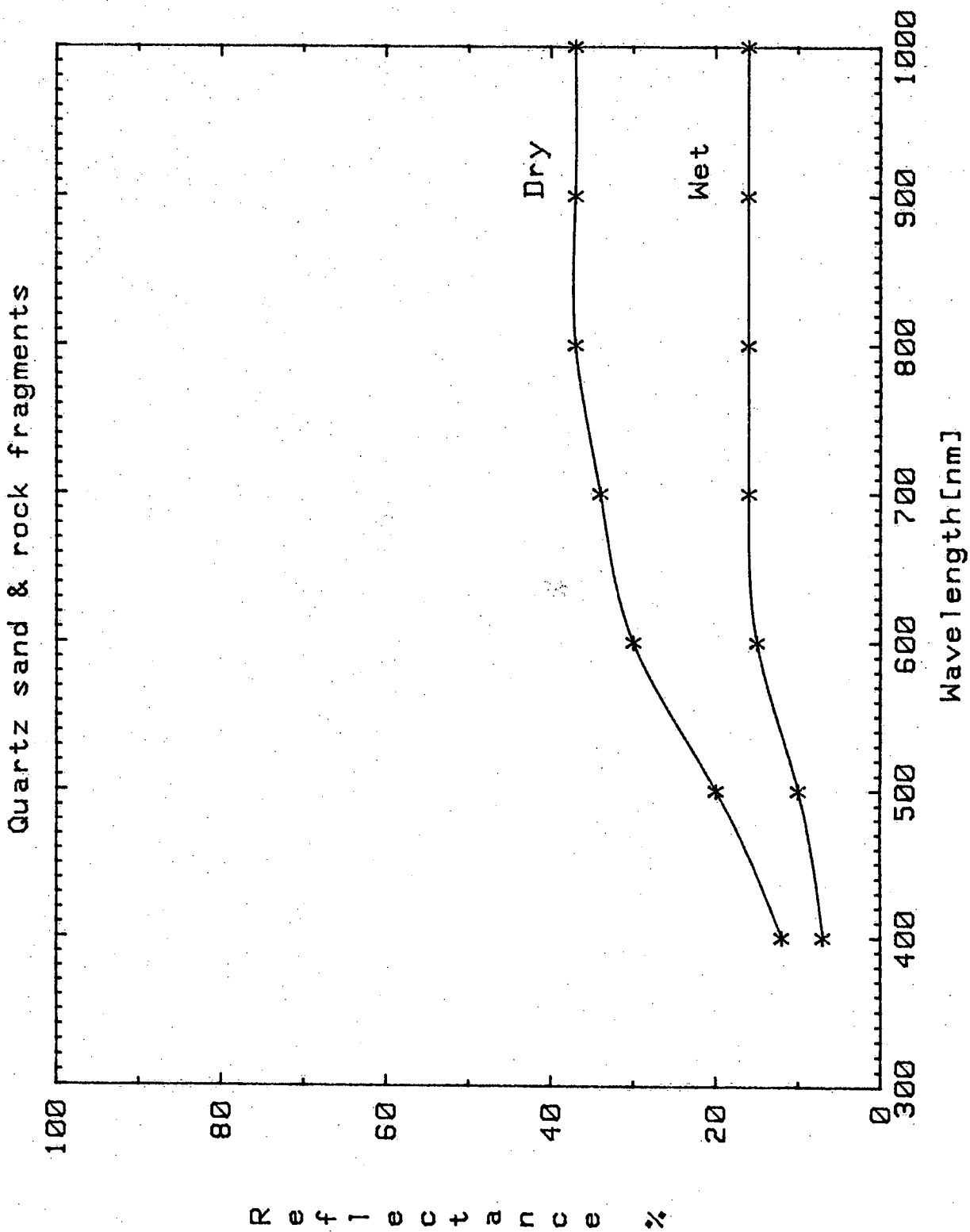
Quartz sand & rock fragments
Dry
Wet
Reflectance %
Wavelength[nm]
100
80
60
40
20
0
300
400
500
600
700
800
900
1000

FIGURE 15.

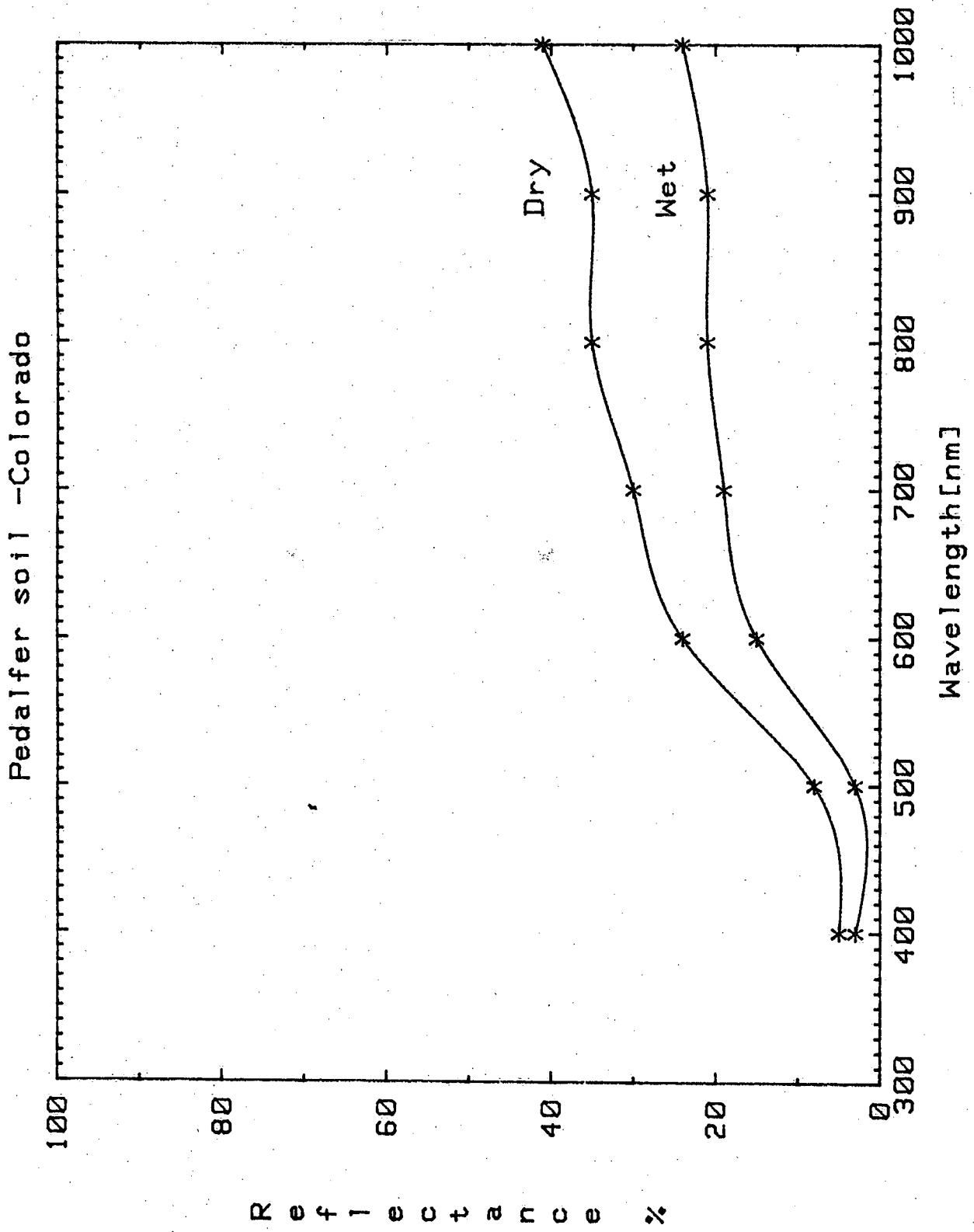
Pedalfer soil -Colorado
Dry
Wet
Reflectance %
Wavelength[nm]
100
80
60
40
20
0
300
400
500
600
700
800
900
1000

FIGURE 16.

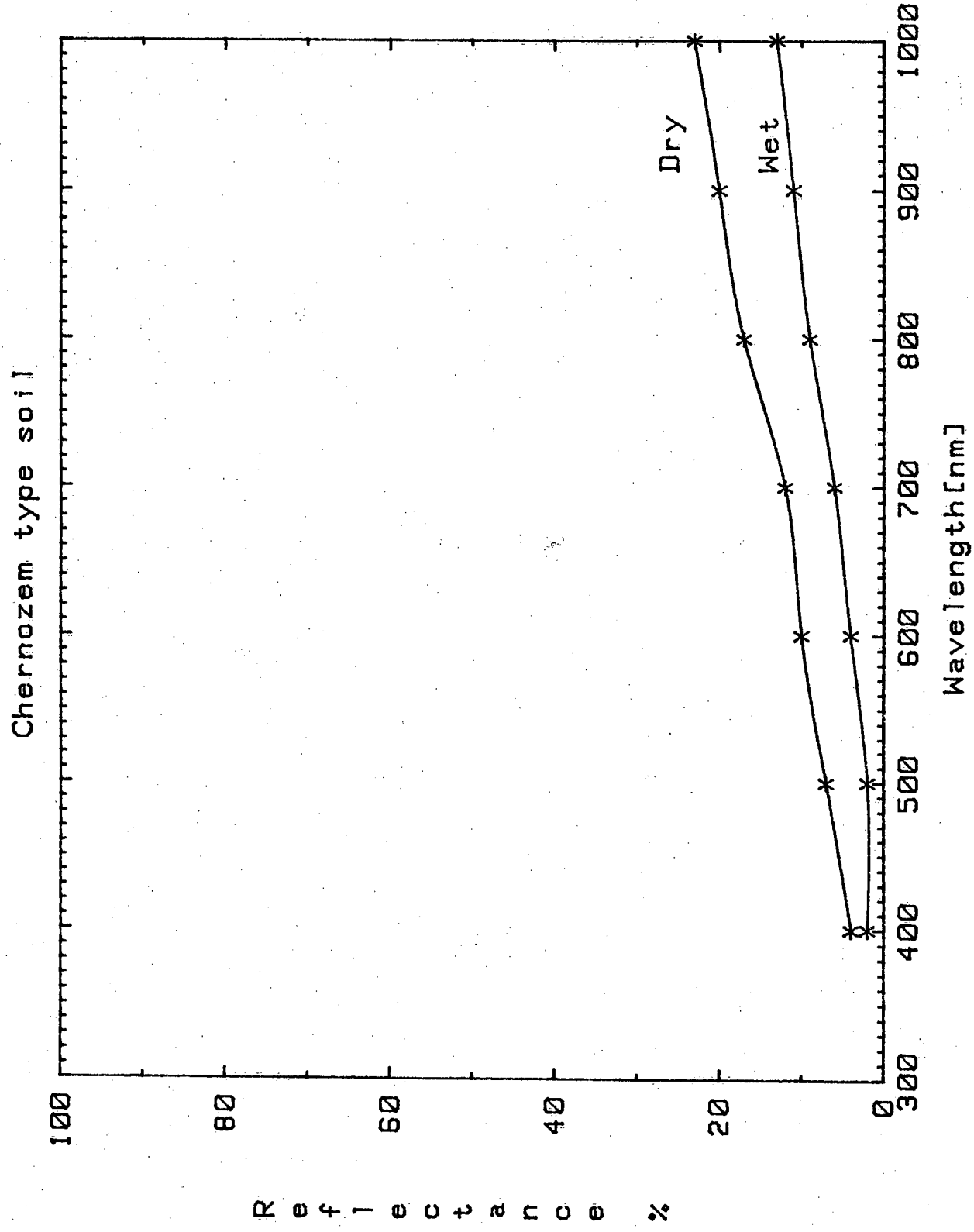
Chernozem type soil
Dry
Wet
Reflectance %
Wavelength[nm]
100
80
60
40
20
0
300
400
500
600
700
800
900
1000

FIGURE 17.

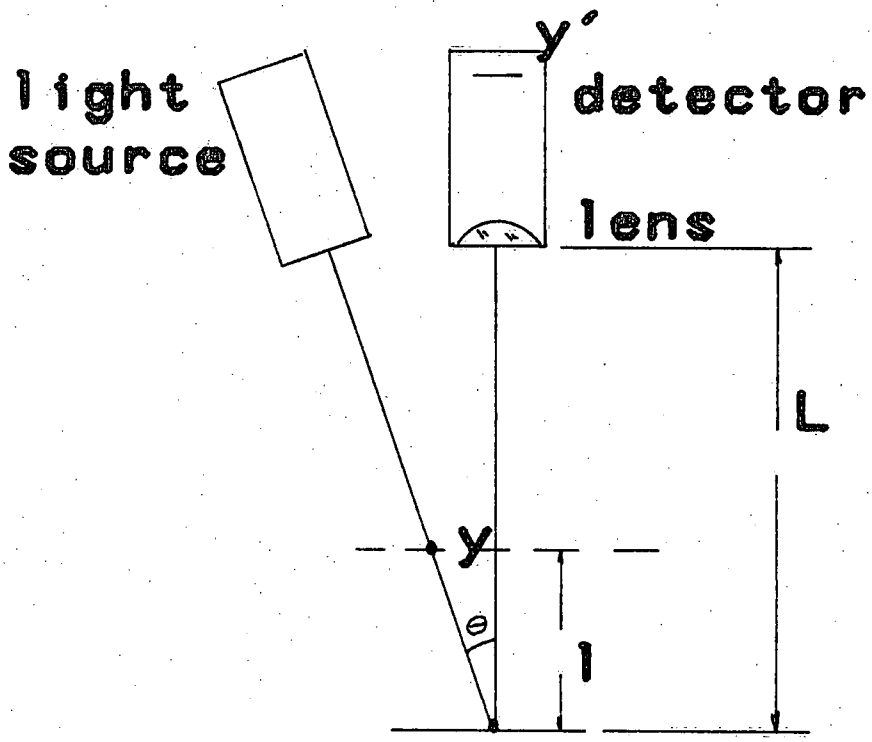

ILLUSTRATION OF SENSOR USING POSITION SENSITIVE DETECTOR